Optimization and mechanism of Acid Orange 7 removal by powdered activated carbon coupled with persulfate by response surface method

Xuxu Wang, Xuebin Hu, Chun Zhao, Zhihua Sun, Huaili Zheng, Junfeng Li and Zhaoyang Wang

ABSTRACT

In this study, powder activated carbon (PAC) utilized to activate peroxydisulfate (PDS) was investigated for decolorization of Acid Orange 7 (AO7). The results indicated a remarkable synergistic effect in the PAC/PDS system. The effect of PAC, PDS dosages and initial pH on AO7 decolorization were studied and the processes followed first-order kinetics. Response surface method with central composite design (CCD) model was utilized to optimize these three factors and analyze the combined interaction. The optimum condition for the decolorization rate of AO7 was analyzed as the following: PAC (0.19 g/L), PDS (1.64 g/L), and initial pH (4.14). Cl^- and SO_4^{2-} showed a promoting effect on AO7 decolorization while HCO_3^- had a slightly inhibiting effect. Quenching experiments confirmed that both sulfate and hydroxyl radicals were the oxidizing species, and the oxidation reaction occurred on the surface of PAC. The results of UV-vis spectrum with 100% decolorization rate and the 50% total organic carbon reduction indicated highly efficient decolorization and mineralization of AO7 in the PAC/PDS system. Finally, the recovery performance of PAC was studied and the result indicated PAC had poor reuse in reactivity.

Key words | peroxydisulfate, powder activated carbon, reaction mechanism, response surface method

Xuxu Wang
Xuebin Hu
Chun Zhao (corresponding author)
Zhihua Sun
Huaili Zheng
State Key Laboratory of Coal Mine Disaster Dynamics and Control,
Chongqing University,
Chongqing 400044,
China
and
Key Laboratory of the Three Gorges Reservoir Region's Eco-Environment, Ministry of Education,
Chongqing University,
Chongqing 400045,
China
E-mail: *pureson@163.com*

Xuxu Wang
Chun Zhao
Zhihua Sun
Junfeng Li
Zhaoyang Wang
College of Water Conservancy and Architectural Engineering,
Shihezi University,
Shihezi 832002,
China

INTRODUCTION

Azo dyes are widely utilized in the textile industry, which play an important role in industry. A great deal of dyeing wastewater is generated by the textile industry, and about 10% of plants discharge into water directly substances that may have carcinogenic or mutagenic effects on human beings (Bakheet *et al.* 2013; Cai *et al.* 2015). Acid Orange 7 (AO7), a typical azo dye which account for about 50% of commercial dyes, is widely utilized in the textile industry (Azam & Hamid 2006; Yusuf *et al.* 2017). Moreover, AO7 has the characteristics of high stability, toxic, and being potentially carcinogenic that make it difficult to dispose of (Brillas & Martinez-Huitle 2015). Thus, the emission of wastewater that contains AO7 will contaminate water and affect the survival of animals continuously without effective treatment. Unfortunately, activated sludge processes and physical adsorption methods (Cai *et al.* 2014) are ineffective to remove AO7 so that it is necessary to search for an effective and economical method to remove such contaminants.

Advanced oxidation processes (AOPs) are regarded as one of the most effective technologies to remove biorefractory organics (Yang *et al.* 2015). Traditional AOPs, based on hydroxyl radicals (·OH, $E_0 = 1.8–2.7$ V) that can oxidize almost all biorefractory organic contaminants quickly without selectivity, have been studied for many years (Yang *et al.* 2015). Recently, more attention has shifted to the sulfate radical ($SO_4^{\cdot-}$) based on AOPs for removing biorefractory organic contaminants, and the oxidants commonly used are peroxydisulfate (PDS) and peroxymonosulfate (PMS), which can be activated to generate $SO_4^{\cdot-}$ ($E_0 = 2.5 \sim 3.1$ V) that oxidizes contaminants quickly but more selectively than ·OH (Chen *et al.* 2016a, 2016b; Huang *et al.* 2017). PDS has a limited ability to degrade contaminants but can

doi: 10.2166/wst.2019.117

decompose contaminants quickly by $SO_4^{\cdot-}$ as in Equations (1) and (2), activated by ultrasound, transition metal ions, heat or several ways combined (Zhang *et al.* 2015; Huang *et al.* 2017). However, the application of ultrasound and heating is limited due to high cost and energy input (Lou *et al.* 2016). Moreover, the use of transition metal ions is also limited because of the potentially adverse effect of secondary pollution on the environment owing to some metal ions (e.g. Co^{2+}) (Huang *et al.* 2017). Therefore, an economic and environmentally friendly method to remove AO7 is needed.

$$S_2O_8^{2-} + UV/US/hv \rightarrow 2SO_4^{\cdot-} \quad (1)$$

$$S_2O_8^{2-} + M^{n+} \rightarrow M^{(n+1)} + SO_4^{\cdot-} + SO_4^{2-} \quad (2)$$

Carbon material is widely utilized as the most versatile adsorbent and catalyst in removing contaminants owing to its enormous specific area and pore volume, porous structure, economy and environmental friendliness. Some studies have utilized activated carbon in activating persulfate and the reaction occurred as in Equations (3) and (4) to remove contaminants such as PEOA, antibiotics, phenol, and 4-chlorophenol (Saputra *et al.* 2013; Kang *et al.* 2016; Huang *et al.* 2017; Guo *et al.* 2018). Recently, more attention has focused on utilizing low-dimensional carbon materials (Chen *et al.* 2017) (such as graphene, carbon nanotubes, nano-biochar) to catalyze persulfate for the degradation of contaminants through the radical pathway (Bekris *et al.* 2017; Kemmou *et al.* 2018). Moreover, some researchers also find that carbon nanotubes can catalyze persulfate for the degradation of 2,4-DCP by the nonradical pathway (Cheng *et al.* 2016; Cheng *et al.* 2017). However, as a cheap and widely used carbon material, there are no reports on using powder activated carbon (PAC) as a catalyst to activate PDS of degrading contaminants. PAC owns a larger specific surface area (BET = 800–1,400 m^2/g) than GAC (BET = 500–900 m^2/g) and has better adsorption and catalytic performance (Saputra *et al.* 2013). PDS may be activated by PAC just like the reactions of Equations (3) and (4) (Yang *et al.* 2015). Thus, in this paper, the objectives were to investigate the decolorization of AO7 in a PAC/PDS system. The effects and interaction of different operating condition parameters on AO7 decolorization were also evaluated and analyzed. Under optimum conditions, the effects of anions were investigated because they are important compositions of the dye wastewater. Moreover, radical species in the PAC/PDS system for removing AO7 were identified. And the UV-vis spectra and total organic carbon (TOC) were monitored to assess the mineralization of AO7. Finally, the stability and reusability of PAC were also researched.

$$GAC_{surface} - OOH + S_2O_8^{2-} \rightarrow GAC_{surface} - OO^{\bullet} + SO_4^{\cdot-} + HSO_4^- \quad (3)$$

$$GAC_{surface} - OH + S_2O_8^{2-} \rightarrow GAC_{surface} - O^{\cdot} + SO_4^{\cdot-} + HSO_4^- \quad (4)$$

METHODS

Experimental procedures and analytical methods

The experiments of AO7 decolorization were carried out in 250 mL Erlenmeyer flasks with magnetic stirring at 300 rpm. The initial pH was adjusted with H_2SO_4 and KOH firstly, then PDS was added into the reactor, which contained AO7 before the reaction, and a certain amount of PAC was quickly added into the reactor. After a fixed interval of reaction of 20 min, 4 mL of the solution was quickly sampled, and filtered with a 0.45 μm membrane for analysis. The UV-vis absorbance of the samples was analyzed at $\lambda = 484$ nm by a 721E Spectrophotometer. UV-vis spectra of AO7 were conducted from 200 to 700 nm using a T6 UV-visible spectrophotometer. The TOC of the samples was quantified by Liqui TDC II analyzer. The morphologies of PAC were examined by scanning electron microscopy (SEM, Tescan Inc., USA). The surface groups of PAC were detected by Boehm titration and Fourier transform infrared spectra (Nicolet iS5 FT-IR spectrometer with KBr Pellet). The key experiments were repeated three times.

Response surface methodology

Central composite design (CCD) and Box-Behnken design are applied in response surface analysis. In this experiment, a CCD statistical model was applied to optimize these operational factors, which included PDS, PAC dosages, and initial pH, and also studied the combined interaction among them. The choice of operational parameters evaluated by response surface methodology (RSM) is based on our preliminary experiments. Each parameter has three levels designed as +1, 0, −1 for high, middle, and low values, respectively. The model consists of a complete factorial design with three replications at the design center, leading to a total of 17 experiments.

RESULTS AND DISCUSSION

A preliminary study of AO7 decolorization by different system

In this work, the decolorization of AO7 was investigated, which considered the adsorption of PAC, the oxidation of PDS, and the oxidation in a PAC/PDS system, which is displayed in Figure 1(a). The results showed that PDS alone had a slight effect on AO7 decolorization and only 8% was oxidized in 120 min, whereas a significant decolorization was observed in the PAC adsorption system, in which 55% was faded in 120 min, which was better than that of other researchers (Zhang *et al.* 2013; Chen *et al.* 2016a, 2016b; Huang *et al.* 2017). Moreover, a removal rate of 98% was observed in the PAC/PDS system, which was clearly better than PDS only and PAC only. Besides, the decolorization of AO7 in these three systems followed first-order kinetics that are presented in Figure 1(b). And the reaction rate constant (k value) in these systems was 6.7×10^{-4}, 0.5×10^{-2} and 3.1×10^{-2} min^{-1}, respectively. It could be seen that the k value in the PAC/PDS system was higher than PAC only and PDS only. Therefore, the result obviously indicated the remarkable synergistic effect of PAC and PDS. Moreover, by analyzing the removal of AO7 in PAC and PAC/PDS processes at different temperatures as displayed in Figure S1 and Table S1 (available with the online version of this paper), we found that the adsorption is a spontaneous process and adsorption capacity would decrease with increasing temperature from 288 to 333 K (Abukhadra *et al.* 2018; Shaban *et al.* 2018). Besides, the k value increased with the increase of temperature indicating that the reaction is an endothermic reaction in the PAC/PDS system (Abukhadra *et al.* 2018; Shaban *et al.* 2018). And the activation energy of the PAC/PDS system was calculated to be 26.68 kJ/mol, which is significantly lower than 81.15 kJ/mol in the base/PMS/AO7 system (Qi *et al.* 2016) indicating that PAC could be an excellent catalyst to activate PDS to decolorize AO7.

Effect of PDS and PAC dosages

The effects of different PDS and PAC dosages were evaluated in the PAC/PDS system. It illustrated that with the raising of PDS dosages, k values accelerated quickly, which is displayed in Figure 2(a). In comparison with the decolorization rate at 0.1 g/L PDS dosages, there was an accelerating effect when PDS dosages increased to 1 g/L. While the increasing trend slightly slowed down as PDS dosages further increased to 4 g/L, where the AO7 decolorization rate was highest (100%). Whereas, when it arrived at 6 g/L PDS dosages, the decolorization rate began to decrease; Yang also had the same results. It might because $SO_4^{\cdot-}$ would quench each other (Equation (5)) (Peyton 1993) and competed with AO7 in the reaction at high dosages of PDS. What's more, $SO_4^{\cdot-}$ might also react with PDS to generate less reactive radicals, e.g. $\cdot S_2O_8^-$ (Equation (6)) (Peyton 1993), at high PDS dosages, which contributed to the decrease of k values. Therefore, it can be seen that suitable PDS dosages could accelerate the reaction while excessive PDS could not accelerate the decolorization of AO7 in

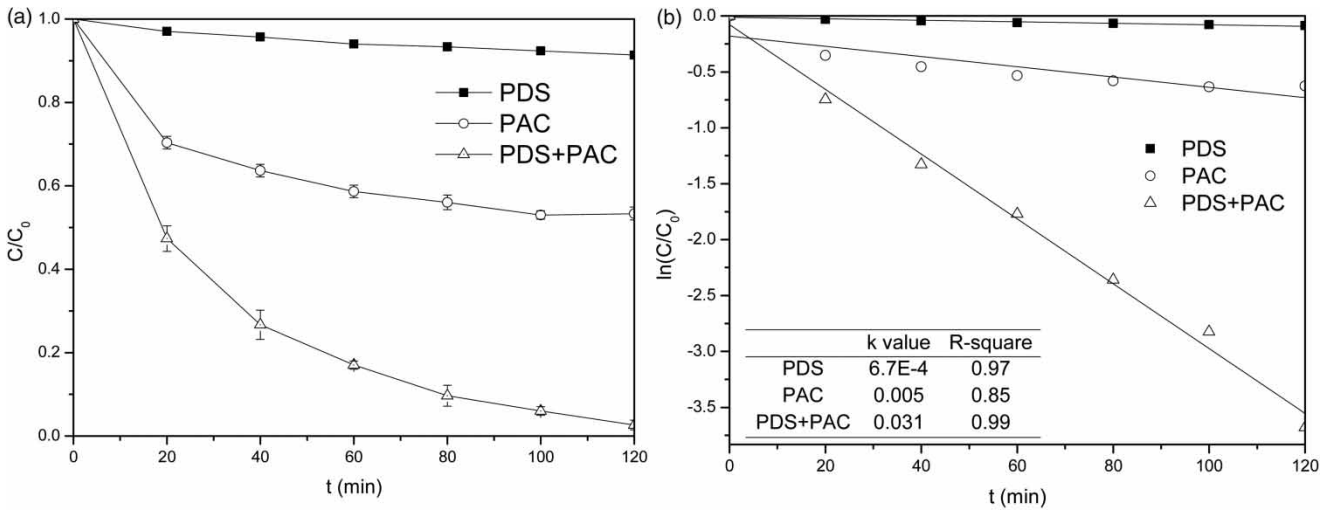

Figure 1 | Decolorization rate (a), and reaction rate (b) of AO7 by different systems (PDS dosage = 6 g/L; PAC dosage = 0.1 g/L; [AO7] = 20 mg/L; V = 250 mL; initial pH = 5.95).

PAC/PDS system.

$$SO_4^{-\bullet} + SO_4^{-\bullet} \rightarrow S_2O_8^{2-} \quad (5)$$

$$SO_4^{-\bullet} + S_2O_8^{2-} \rightarrow S_2O_8^{2-\bullet} + SO_4^{2-} \quad (6)$$

The effect of different PAC dosages on AO7 decolorization in the PAC/PDS system was evaluated and is displayed in Figure 2(b). It illustrated that with the increase of PAC dosages, the AO7 decolorization rate was observed to be faster in the PAC/PDS system. Compared with the AO7 decolorization rate at 0.05 g/L PAC dosages, there was an accelerating effect when PAC dosages increased to 0.3 g/L. The reason might be that higher PAC dosages increased the BET, which increased the amount of active sites for adsorption and the catalytic reaction. The reaction speed had slowed down markedly when PAC dosages further increased from 0.3 g/L (k value $= 6.03 \times 10^{-2}$ min^{-1}) to 0.4 g/L (k value $= 6.10 \times 10^{-2}$ min^{-1}). This was probably because the reaction rate was limited by the reaction rate of the radical.

Effect of initial pH

The initial pH, which was regarded as an important factor on AO7 decolorization, was also evaluated and demonstrated. As shown in Figure 2(c), the decolorization of AO7 at the lowest initial pH of 3 was slightly higher than that at pH of 7, 11 in the PAC/PDS system and decreased with the increase of initial pH. The initial pH could affect the charge-carrying state of PAC. When pH < pH_{PZC} (potential of zero charge), PAC owned a positive surface charge that would adsorb AO7 ($pK_{a1} = 8.26$) which owned a negative surface charge in the opposite condition (Reymond & Kolenda 1999). Thus, the decolorization of AO7 by PAC was also evaluated and the fastest decolorization rate of

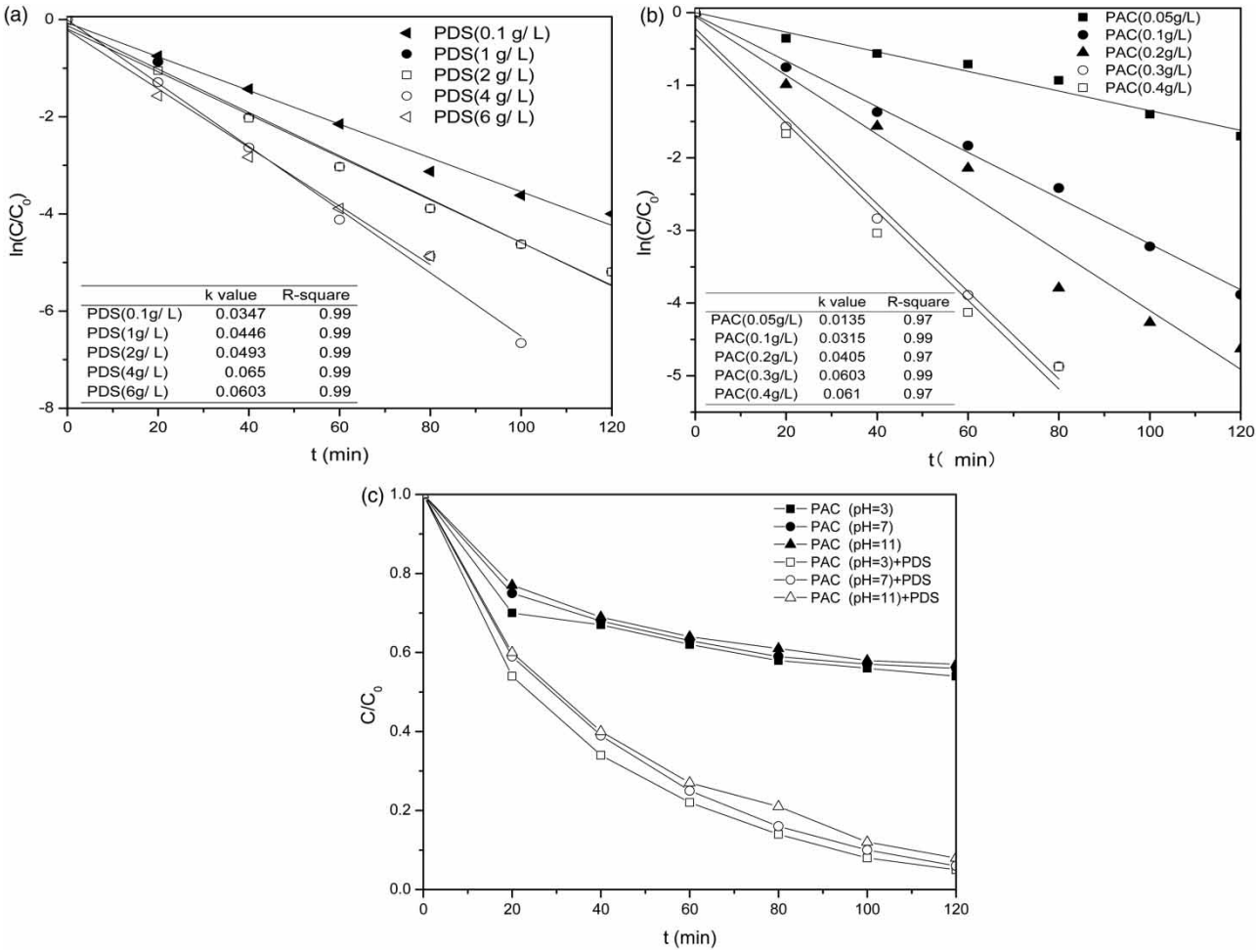

Figure 2 | Effects of PDS dosages on the decolorization of AO7 at the fixed PAC dosage = 0.3 g/L (a), effects of PAC dosage on the decolorization of AO7 at the fixed PDS dosage = 6 g/L (b), and initial pH on the decolorization of AO7 (c) in the PAC/PDS system ([AO7] = 20 mg/L; V = 250 mL).

AO7 also occurred at pH 3 as shown in Figure 2(c). Moreover, the pH_{PZC} of PAC used in this study was 6.1. Under acidic conditions, PAC owned a more positive surface charge, adsorbing more anionic AO7 and accelerating the decolorization of AO7. Whereas, under alkaline conditions, PAC owned a negative surface charge that excluded AO7 by static repulsion. Moreover, $SO_4^{-\bullet}$ (4 s) may be converted to ·OH (20 ns) which has a very short existence time and a very poor reactivity with AO7 opposing to $SO_4^{-\bullet}$, as illustrated by Equation (7) (Lee *et al.* 2013). The change of pH shown in Figure S2 (available online) also confirmed this. Overall, an acidic condition would slightly accelerate the decolorization of AO7 while an alkaline condition had a slight inhibitory effect.

$$SO_4^{-\bullet} + OH^- \rightarrow SO_4^{2-} + \bullet OH \quad (7)$$

Optimization of PAC, PDS dosages and initial pH by using RSM

The effect of three significant parameters on the decolorization of AO7 was optimized using RSM as given in Table S2 (available online). Furthermore, their responses were predicted and the optimum conditions for decolorization were also determined. The results of the analysis of variance (ANOVA) of the response surface quadratic analyses and model terms are shown in Table 1. From the ANOVA results, the model F value 140.17 indicated that the linear model with the curvature term was statistically significant. And the values of 'lack of fit' (F value) were less than 0.05, which implied that the lack of fit was not significant relative to the pure error. Moreover, the coefficient of determination (R^2) of the model was 0.9642, and the adjusted R^2 was 0.9838. Both of the values are very near to 1.0, indicating a high correlation between the actual and the predicted values as shown in Figure S3 (available online) (Lim *et al.* 2013; Selvakumar *et al.* 2013). Thus, it was a good predictor of response and could be used to predict the optimal value. By regression analysis, a quadratic model was predicted as in the following equation: The removal of AO7=20.26681-2.23275 × pH + 47.33064 × PDS + 490.69493 × PAC + 13.90476 × pH × PAC-103.52941 × PDS × PAC-9.02522 × PDS^2-1005.27954 × PAC^2.

By using the quadratic model, a removal of 100% was predicted, the optimum condition for the decolorization rate of AO7 was found to be as follows: PAC (0.19 g/L), PDS (1.64 g/L), and initial pH (4.14). A confirmatory experiment was performed three times in order to test the suitability of the model and a removal of 100% was obtained that illustrated the reliability of the model. Moreover, the interactions of the three parameters were also analyzed by RSM. Figure 4 indicates the Contour plot of percent removal of AO7 as a function of two parameters. The elliptical shape of the curve indicated good interaction between the two variables and the circular shape indicates no interaction (Oladipo & Gazi 2014). From Figure 3, a relatively significant interaction between PDS and PAC was observed. It showed that the decolorization rate of AO7 increased slightly with the increase of PDS and PAC concentrations. A relative interaction between initial pH and PAC was also observed and there was also a relative interaction.

Table 1 | Variance analysis of regression equation

Source	df	Sum of squares	Mean square	F-value	Prob > F	Significant
Model	7	5,378.09	768.30	140.17	<0.0001	Y
A-pH	1	34.36	34.36	6.27	0.0336	Y
B-PDS	1	1,539.08	1,539.08	280.80	<0.0001	Y
C-PAC	1	2,862.73	2,862.73	522.29	<0.0001	Y
AC	1	106.58	106.58	19.44	0.0017	Y
BC	1	348.48	348.48	63.58	<0.0001	Y
B^2	1	266.07	266.07	48.54	<0.0001	
C^2	1	200.09	200.09	36.50	0.0002	
Residual	9	49.33	5.48			
Lack of fit	7	48.28	6.90	13.18	0.0723	N
Pure error	1.05	2	0.52			
Cor total	16	5427.42				

$R^2 = 0.9642$, $R^2_{adj} = 0.9838$.

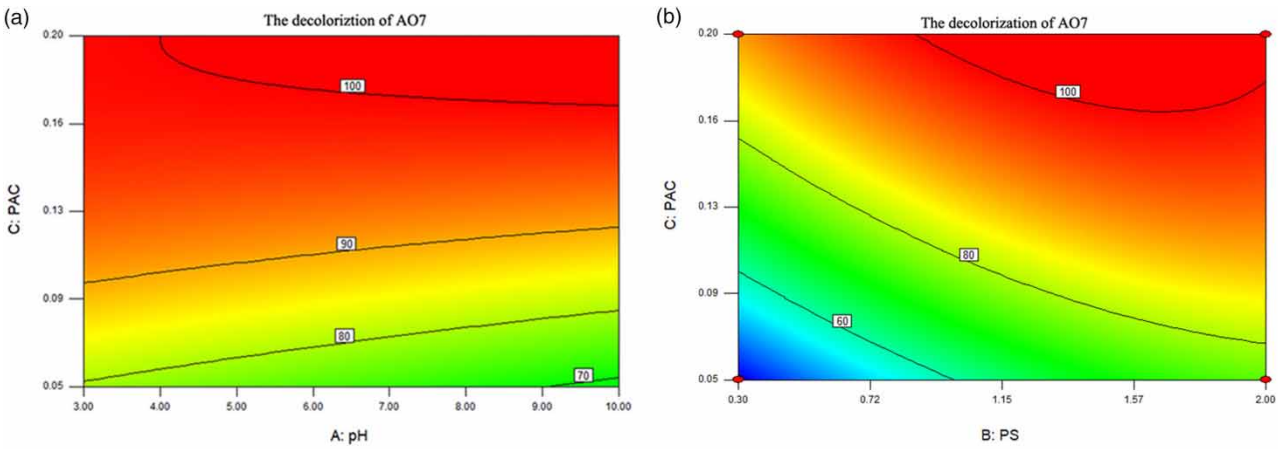

Figure 3 | Contour plot showing the interactive effect of pH and PAC (a), PAC and PDS (b) on decolorization of AO7.

Effect of inorganic salt in the dyeing wastewater

Effect of HCO_3^- dosages

The effect of HCO_3^- on AO7 decolorization was researched as shown in Figure 4(a). It illustrated that with increasing dosages of HCO_3^-, it inhibited AO7 degradation in the PAC/PDS system. The values decreased from 2.73×10^{-2} to $2.15\times10^{-2}\,min^{-1}$ with the dosages of HCO_3^- increasing from 1 to 100 mM. The addition of carbonate reacted with H^+ in solution, which would increase the pH value, which is shown in Figure S4 (available online), that interfered with the decolorization of AO7 (Canonica *et al.* 2005). Moreover, the decrease in AO7 decolorization might be attributed to the conversion of $SO_4^{-\bullet}$ to less reactive radical species, such as $CO_3^{-\bullet}$ (E_0=1.7 V) as in Equation (8) (Neppolian *et al.* 2002).

$$SO_4^{-\bullet} + HCO_3^- \rightarrow SO_4^{2-} + H^+ + CO_3^{-\bullet} \quad (8)$$

Effect of SO_4^{2-}

The effect of SO_4^{2-} on AO7 decolorization in the PAC/PDS system was researched as displayed in Figure 4(b). It illustrated that with the increasing dosages of SO_4^{2-}, AO7 decolorization accelerated gradually. Moreover, when higher dosages of SO_4^{2-} were added, the k values gradually increased from 2.72×10^{-2} to $4.20\times10^{-2}\,min^{-1}$. It could be seen that the effect of SO_4^{2-} on AO7 decolorization in the activated PDS process was consistent with that previously reported (Neppolian *et al.* 2002; Rao *et al.* 2014). On the one hand, a higher SO_4^{2-} dosage could prevent the quenching and transformation of $SO_4^{-\bullet}$ as in Equation (6) and (7). On the other hand, it was reported previously that a higher dosage of SO_4^{2-} could increase the ion strength and induce the dye dimerization in the solution (Chen *et al.* 2016a, 2016b). The aggregation of dye molecules would increase the extent of adsorption of AO7 on the PAC surface. Thus, the addition of SO_4^{2-} could raise the adsorption of AO7 on the PAC surface for AO7 decolorization induced by the radical species activated by the oxygen functional groups onto PAC.

Effect of Cl^-

NaCl was a common dying agent that was utilized extensively to accelerate the dyeing process. Thus, dye wastewater always contained a large amount of salt. The effect of Cl^- concentration on AO7 decolorization was researched as shown in Figure 4(c). With the increase of Cl^- concentration, k values of AO7 were significantly increased from 2.72×10^{-2} to $5.20\times10^{-2}\,min^{-1}$, which was similar to previous reports (Anipsitakis *et al.* 2006; Chen *et al.* 2016a, 2016b). Previous reports had proposed that excessive dosage of Cl^- could accelerate the decolorization of contaminants in SR-AOPs, and that it might react with $SO_4^{-\cdot}$ to generate chlorine radical species (Cl·, $Cl_2^{-\cdot}$) and other strong oxide species (Cl_2, HClO) just as in Equations (9)–(13), which were mainly responsible for the accelerating effect. Moreover, it would further react with PDS to increase the overall amount of $SO_4^{-\cdot}$ (Anipsitakis *et al.* 2006; Chen *et al.* 2016a, 2016b). Hence, we completed the following experiments as shown in Figure S5 (available online) to verify the occurrence of

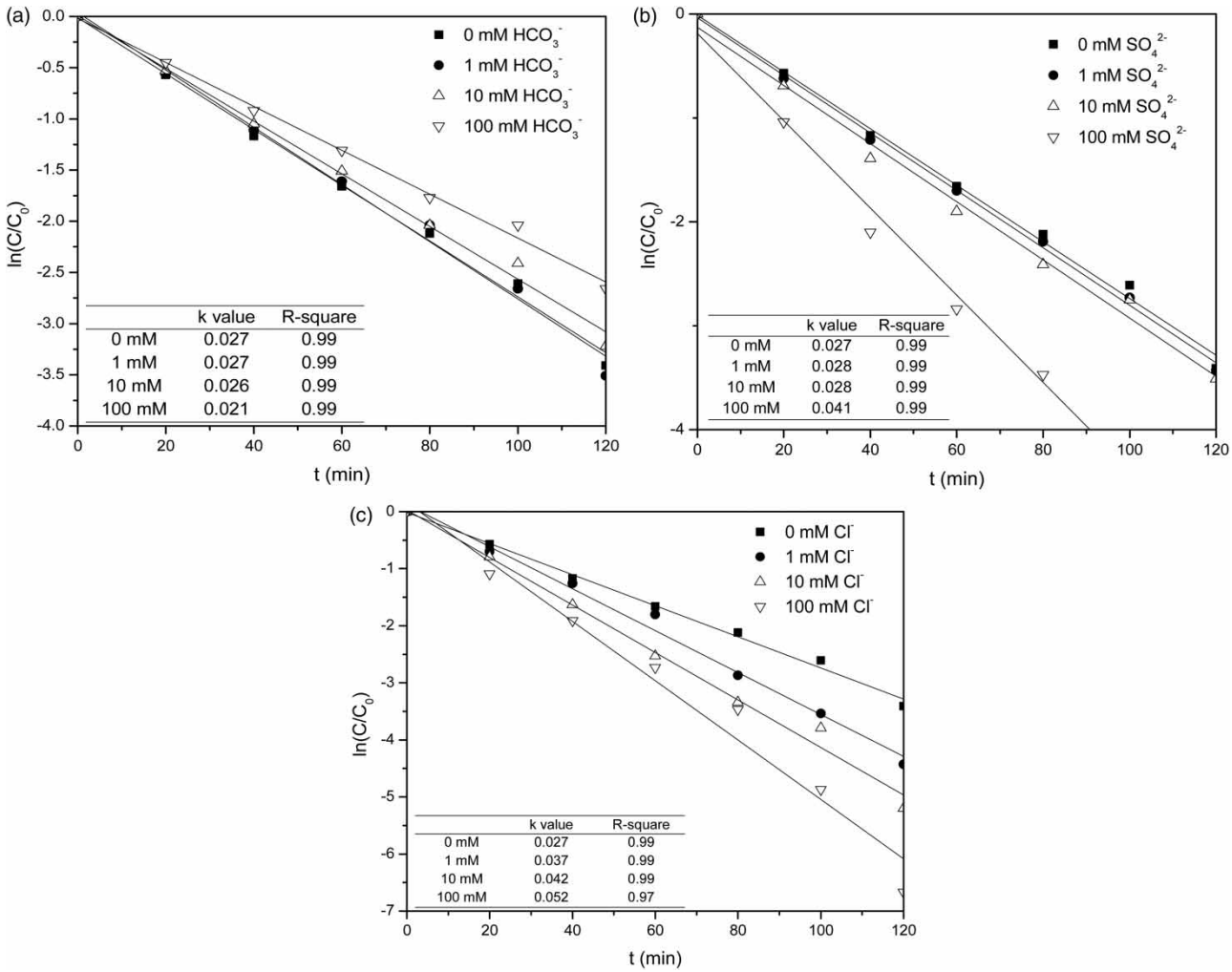

Figure 4 | Effects of HCO_3^- dosages (a), SO_4^{2-} dosages (b), and Cl^- dosages (c) on the decolorization of AO7 in PAC/PDS system (PAC dosage = 0.19 g/L; PDS dosage = 1.64 g/L; initial pH = 4.14; [AO7] = 20 mg/L; V = 250 mL).

the above reactions in this system and the main effect species in the decolorization of AO7 at high Cl^- dosages. We introduced excessive phenol, which was scavenging $SO_4^{-\cdot}$, and the result displayed that the addition of phenol almost completely inhibited AO7 decolorization. Thus, it indicated that the reactions were not taking place in this system. Moreover, we further introduced NH_4^+, which reacted with HClO to generate less reactive chloramines (Lou *et al.* 2013), and the result confirmed that HClO did not participate in AO7 decolorization and the reactions did not occur. Thus, considering the influence on AO7 adsorption on PAC, we researched the effect of Cl^- on AO7 adsorption on PAC finally as displayed in Figure S6 (available online). It was shown that with the increase of Cl^- dosages, the AO7 decolorization rate slightly accelerated, which instructed that the promotion of Cl^- was attributed to the adsorption of PAC.

$$SO_4^{-\bullet} + Cl^- \rightarrow SO_4^{2-} + Cl\bullet \quad (9)$$

$$Cl\bullet + Cl^- \rightarrow Cl_2^{\bullet-} \quad (10)$$

$$Cl\bullet + Cl\bullet \rightarrow Cl_2 \quad (11)$$

$$Cl_2^{\bullet-} + Cl_2^{\bullet-} \rightarrow Cl_2 + 2Cl^- \quad (12)$$

$$Cl_2 + H_2O \rightarrow HClO + Cl^- + H^+ \quad (13)$$

UV-vis spectra and the TOC removal

In order to figure out the change of structural characteristics of AO7 during the decolorization process in the PAC/PDS

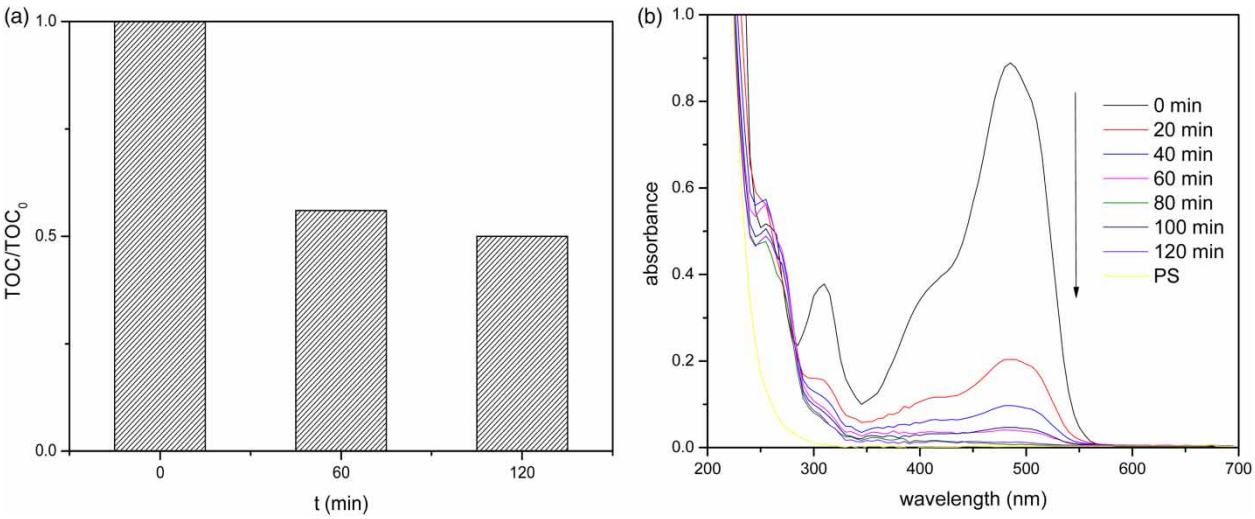

Figure 5 | UV–vis spectra (a) and TOC removal (b) of AO7 decolorization in the PAC/PDS system (PAC dosage = 0.19 g/L; PDS dosage = 1.64 g/L; initial pH = 4.14; [AO7] = 20 mg/L; V = 250 ml).

system, samples were taken every 20 minutes and monitored in the spectrum of AO7. AO7 consists of an azo bond, hydrazone form, naphthalene ring, and a benzene ring basically, which accounted for the four apparent peaks at 484, 430, 310, and 229 nm, respectively. The maximum absorption wavelength for AO7 was determined to be 484 nm, which accounts for the orange color of the solution and can be attributed to the azo bond (Bauer *et al.* 2001). The decolorization of AO7 over 120 min is shown in Figure 5(a). Moreover, the UV-vis spectrum of PDS in the distilled water was also detected. It was apparent that characteristic peaks at 484 nm and 310 nm declined and the removal efficiency of these peaks was about 90% and 30% in 120 min, respectively. While the 229 nm absorption band was still present, a high position proving the highly refractory nature of the benzene ring. Thus, it could be speculated that AO7 might be partly mineralized in PAC/PDS system. In order to demonstrate whether AO7 was mineralized or not, the TOC variation was monitored as shown in Figure 5(b). TOC gradually decreased during AO7 decolorization and the removal efficiency at 60 min and 120 min reaches 44% and 50%, respectively. Above all, it proved that PDS activated by PAC could break up the AO7 molecular structure and mineralize AO7 effectively.

The proposed reaction mechanism

PDS might be activated by PAC to generate $SO_4^{-\bullet}$, as mentioned above (Equations (3) and (4)). Moreover, the presence of $SO_4^{-\bullet}$ could result in radical interconversion reactions to produce •OH (Equation (14)). It has been reported that both $SO_4^{-\bullet}$ and •OH have strong oxidizing property in removing organic dyes (Liang *et al.* 2007).

$$SO_4^{-\bullet} + H_2O \rightarrow \bullet OH + SO_4^{2-} + H^+ \quad (14)$$

Therefore, both $SO_4^{-\bullet}$ and •OH are possibly responsible for the decolorization of AO7 in the PAC/PDS system. In order to identify the dominating oxidizing species working in the experiment, methanol, tertbutanol, and phenol, which were commonly used as free radical inhibitors, were utilized. Methanol was highly reactive with both $SO_4^{-\bullet}$ and •OH with k values of 9.7×10^8 and $3.2 \times 10^6\ M^{-1}s^{-1}$, respectively. Whereas tertbutanol was also an effective quenching agent for •OH while reacting much more slowly with $SO_4^{-\bullet}$ such that the k values were $(3.8–7.6) \times 10^8$ and $(4–9.1) \times 10^5\ M^{-1}s^{-1}$, respectively. Besides, phenol was another strong quencher radical ($k_{SO4/phenol} = 8.8 \times 10^9\ M^{-1}s^{-1}$, $k_{OH/phenol} = 6.6 \times 10^9\ M^{-1}s^{-1}$) that showed a strong inhibiting effect on $SO_4^{-\bullet}$ and •OH (Ziajka & Pasiuk-Bronikowska 2005). As shown in Figure 6, when methanol or tertbutanol were added into the PAC/PDS system, there was only a slight inhibitory effect on AO7 decolorization. When phenol was added into the system, the reaction of AO7 decolorization slowed down and the inhibiting effect was remarkable. Methanol and tertbutanol were relatively hydrophilic that could compete with $SO_4^{-\bullet}$ and •OH radicals taking place in the aqueous solution even though they couldn't accumulate on the PAC surface to a significant extent. While phenol is more hydrophobic than methanol and tertbutanol, thus, it is easier to approach carbon surface to prevent the activation of PDS by oxygen surface function groups which were distributed in

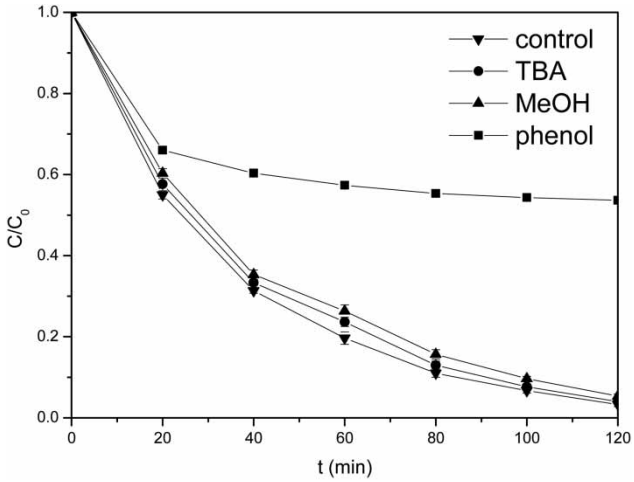

Figure 6 | Effect of free radical inhibitors on the decolorization of AO7 in PAC/PDS system (PAC dosage = 0.19 g/L; PDS dosage = 1.64 g/L; initial pH = 4.14; [AO7] = 20 mg/L; V = 250 mL; c(MA)/[AO7] = c(TBA)/[AO7] = 1000/1; c(phenol)/[AO7] = 100/1).

the carbon material surface (Chen *et al.* 2016a, 2016b). Therefore, the areas of free radicals-induced degradation of AO7 were most likely taking place on the surface of the PAC. Moreover, $SO_4^{\cdot-}$ was mainly responsible for the AO7 degradation in PAC/PDS system.

Reusability and recovery performance of PAC

A reuse experiment was conducted to detect the recovery performance of PAC four times, as displayed in Figure S7 (available online). The decolorization efficiencies of AO7 removal for four reuse cycles gradually decreased and were 97%, 90%, 79%, 53%, respectively. Also, the morphologies and functional groups of PAC before and after reaction were inspected by SEM, FT-IR, and Boehm titration. As displayed in Figure S8 and Table S3 (available online), the SEM images of virgin PAC appear to be rough and dusty, whereas the oxidation of PDS resulted in a relatively neat surface on the PAC. Moreover, after the reaction, the decrease of the peak at 3,420 cm^{-1} and the increase of the asymmetrical band at 1,110 cm^{-1} revealed the increase of acid groups and the C-O-C band, which resulted from the oxidation of the C = O band by PDS (Li *et al.* 2017) It was consistent with the results of change of the functional groups on the PAC surface by Boehm titration. The results were similar to previous studies reporting that the removal rate gradually decreased with the increase of reuse cycles of AC owing to the decrease in surface area of AC and the consumption of oxygen-containing alkaline functional groups (Li *et al.* 2017), which indicated that AC may not actually be a catalyst for electron transfer media, but a PS-activated initiator (Liu *et al.* 2018). The deactivation of PAC in the PAC/PDS system could be due to the exhaustion of electron-donating residues on the PAC, which can trigger PDS into $SO_4^{\cdot-}$. Besides, the incomplete removal of AO7 and intermediate products adsorbed on the surface of PAC inhibited the interaction between PDS and PAC. But when PAC was reused three times the removal rate of AO7 was obviously decreased, which was different from other researches. This was mainly because of the difficulty of recovery and serious problems with loss of PAC, which was also a problem that restricted the development of PAC in the field of water treatment.

CONCLUSIONS

The present work demonstrates that PAC can not only remove AO7 through adsorption but also catalyzes PDS, forming $SO_4^{\cdot-}$ and ·OH to remove AO7. The decolorization processes follow first-order kinetics. Moreover, univariate analysis showed that the decolorization efficiency increased as the PDS and PAC dosages increased. The decolorization rate of AO7 is highest in acidic conditions and the maximum removal is found at pH 3. The results of RSM show PDS, PAC dosages, and initial pH have remarkable interaction. The optimum condition through RSM is found to be as follows: PAC (0.19 g/L), PDS (1.64 g/L), and initial pH (4.14). Addition of Cl^- and SO_4^{2-} accelerated AO7 decolorization while the presence of HCO_3^- slightly retarded AO7 decolorization. A maximum of 100% color removal and 50% TOC reduction confirm the mineralization of AO7 in PAC/PDS system. The efficiency of AO7 removal in four reuse cycles, which gradually decreased, indicates that PAC was partially deactivated in the PAC/PDS system. Nevertheless, this experiment is just under optimal pH but did not consider AO7 removal efficiency under the condition of normal pH and raw water from a textile factory. In addition, the specific degradation process of AO7 also requires further study in the PAC/PDS system. Moreover, this system is expected to be used in the field of printing and dyeing wastewater treatment and emergency water treatment.

ACKNOWLEDGEMENTS

This work was financially supported by the Fundamental Research Funds for the Central Universities of China (No. 2018CDYJSY0055), the National Natural Science

Foundation of China (No. 51308563), Graduate Research and Innovation Foundation of Chongqing of China (No. CYS18030), and the Frontier Interdisciplinary Training Project of Fundamental Research Funds for the Central Universities of China (No. 2018CDQYCH0053).

REFERENCES

Abukhadra, M. R., Rabia, M., Shaban, M. & Verpoort, F. 2018 Heulandite/polyaniline hybrid composite for efficient removal of acidic dye from water; kinetic, equilibrium studies and statistical optimization. *Adv. Powder Technol.* **29**, 2501–2511.

Anipsitakis, G. P., Dionysiou, D. D. & Gonzalez, M. A. 2006 Cobalt-mediated activation of peroxymonosulfate and sulfate radical attack on phenolic compounds. Implications of chloride ions. *Environ. Sci. Technol.* **40**, 1000–1007.

Azam, A. & Hamid, A. 2006 Effects of gap size and UV dosage on decolorization of CI Acid Orange 7 by UV/H_2O_2 process. *J. Hazard. Mater.* **133**, 167–171.

Bakheet, B., Yuan, S., Li, Z., Wang, H., Zuo, J., Komarneni, S. & Wang, Y. 2013 Electro-peroxone treatment of Orange II dye wastewater. *Water Res.* **47**, 6234–6243.

Bauer, C., Jacques, P. & Kalt, A. 2001 Photooxidation of an azo dye induced by visible light incident on the surface of TiO_2. *J. Photochem. Photobiol. A* **140**, 87–92.

Bekris, L., Frontistis, Z., Trakakis, G., Sygellou, L., Galiotis, C. & Mantzavinos, D. 2017 Graphene: a new activator of sodium persulfate for the advanced oxidation of parabens in water. *Water Res.* **126**, 111–121.

Brillas, E. & Martinez-Huitle, C. A. 2015 Decontamination of wastewaters containing synthetic organic dyes by electrochemical methods. An updated review. *Appl. Catal. B-Environ.* **166**, 603–643.

Cai, C., Zhang, H., Zhong, X. & Hou, L. 2014 Electrochemical enhanced heterogeneous activation of peroxydisulfate by Fe-Co/SBA-15 catalyst for the degradation of Orange II in water. *Water Res.* **66**, 473–485.

Cai, C., Zhang, H., Zhong, X. & Hou, L. 2015 Ultrasound enhanced heterogeneous activation of peroxymonosulfate by a bimetallic Fe-Co/SBA-15 catalyst for the degradation of Orange II in water. *J. Hazard. Mater.* **283**, 70–79.

Canonica, S., Kohn, T., Mac, M., Real, F. J., Wirz, J. & Von Gunten, U. 2005 Photosensitizer method to determine rate constants for the reaction of carbonate radical with organic compounds. *Environ. Sci. Technol.* **39**, 9182–9188.

Chen, J., Hong, W., Huang, T., Zhang, L., Li, W. & Wang, Y. 2016a Activated carbon fiber for heterogeneous activation of persulfate: implication for the decolorization of azo dye. *Environ. Sci. Pollut. Res.* **23**, 18564–18574.

Chen, J., Qian, Y., Liu, H. & Huang, T. 2016b Oxidative degradation of diclofenac by thermally activated persulfate: implication for ISCO. *Environ. Sci. Pollut. Res.* **23**, 3824–3833.

Chen, J., Wang, B. & Hu, Y. 2017 An existence criterion for low-dimensional materials. *J. Mech. Phys. Solids* **107**, 451–468.

Cheng, X., Guo, H., Zhang, Y., Liu, Y., Liu, H. & Yang, Y. 2016 Oxidation of 2,4-dichlorophenol by non-radical mechanism using persulfate activated by Fe/S modified carbon nanotubes. *J. Colloid. Interf. Sci.* **469**, 277–286.

Cheng, X., Guo, H., Zhang, Y., Wu, X. & Liu, Y. 2017 Non-photochemical production of singlet oxygen via activation of persulfate by carbon nanotubes. *Water Res.* **113**, 80–88.

Guo, Y., Zeng, Z., Zhu, Y., Huang, Z., Cui, Y. & Yang, J. 2018 Catalytic oxidation of aqueous organic contaminants by persulfate activated with sulfur-doped hierarchically porous carbon derived from thiophene. *Appl. Catal. B-Environ.* **220**, 635–644.

Huang, T., Chen, J., Wang, Z., Guo, X. & Crittenden, J. C. 2017 Excellent performance of cobalt-impregnated activated carbon in peroxymonosulfate activation for acid orange 7 oxidation. *Environ. Sci. Pollut. Res.* **24**, 9651–9661.

Kang, J., Duan, X., Zhou, L., Sun, H., Tadé, M. O. & Wang, S. 2016 Carbocatalytic activation of persulfate for removal of antibiotics in water solutions. *Chem. Eng. J.* **288**, 399–405.

Kemmou, L., Frontistis, Z., Vakros, J., Manariotis, I. D. & Mantzavinos, D. 2018 Degradation of antibiotic sulfamethoxazole by biochar-activated persulfate: factors affecting the activation and degradation processes. *Catal. Today* **313**, 128–133.

Lee, Y., Lo, S., Kuo, J. & Huang, C. 2013 Promoted degradation of perfluorooctanic acid by persulfate when adding activated carbon. *J. Hazard. Mater.* **261**, 463–469.

Li, J., Lin, H., Zhu, K. & Zhang, H. 2017 Degradation of Acid Orange 7 using peroxymonosulfate catalyzed by granulated activated carbon and enhanced by electrolysis. *Chemosphere* **188**, 139–147.

Liang, C., Wang, Z. & Bruell, C. J. 2007 Influence of pH on persulfate oxidation of TCE at ambient temperatures. *Chemosphere* **66**, 106–113.

Lim, C. K., Bay, H. H., Aris, A., Abdul Majid, Z. & Ibrahim, Z. 2013 Biosorption and biodegradation of Acid Orange 7 by Enterococcus faecalis strain ZL: optimization by response surface methodological approach. *Environ. Sci. Pollut. Res.* **20**, 5056–5066.

Liu, Z., Zhao, C., Wang, P., Zheng, H., Sun, Y. & Dionysiou, D. D. 2018 Removal of carbamazepine in water by electro-activated carbon fiber-peroxydisulfate: comparison, optimization, recycle, and mechanism study. *Chem. Eng. J.* **343**, 28–36.

Lou, X., Guo, Y., Xiao, D., Wang, Z., Lu, S. & Liu, J. 2013 Rapid dye degradation with reactive oxidants generated by chloride-induced peroxymonosulfate activation. *Environ. Sci. Pollut. Res.* **20**, 6317–6323.

Lou, X., Xiao, D., Fang, C., Wang, Z., Liu, J., Guo, Y. & Lu, S. 2016 Comparison of UV/hydrogen peroxide and UV/peroxydisulfate processes for the degradation of humic acid in the presence of halide ions. *Environ. Sci. Pollut. Res.* **23**, 4778–4785.

Neppolian, B., Choi, H. C., Sakthivel, S., Arabindoo, B. & Murugesan, V. 2002 Solar light induced and TiO_2 assisted degradation of textile dye reactive blue 4. *Chemosphere* **46**, 1173–1181.

Oladipo, A. A. & Gazi, M. 2014 Enhanced removal of crystal violet by low cost alginate/acid activated bentonite composite beads:

optimization and modelling using non-linear regression technique. *J. Water Process Eng.* **2**, 43–52.

Peyton, G. R. 1993 The free-radical chemistry of persulfate-based total organic-carbon analyzers. *Mar. Chem.* **41**, 91–103.

Qi, C., Liu, X., Ma, J., Lin, C., Li, X. & Zhang, H. 2016 Activation of peroxymonosulfate by base: implications for the degradation of organic pollutants. *Chemosphere* **151**, 280–288.

Rao, Y. F., Qu, L., Yang, H. & Chu, W. 2014 Degradation of carbamazepine by Fe(II)-activated persulfate process. *J. Hazard. Mater.* **268**, 23–32.

Reymond, J. P. & Kolenda, F. 1999 Estimation of the point of zero charge of simple and mixed oxides by mass titration. *Powder Technol.* **103**, 30–36.

Saputra, E., Muhammad, S., Sun, H. & Wang, S. 2013 Activated carbons as green and effective catalysts for generation of reactive radicals in degradation of aqueous phenol. *RSC Adv.* **3**, 21905–21910.

Selvakumar, S., Manivasagan, R. & Chinnappan, K. 2013 Biodegradation and decolourization of textile dye wastewater using *Ganoderma lucidum*. *3 Biotech* **3**, 71–79.

Shaban, M., Abukhadra, M. R., Mohamed, A. S., Shahien, M. G. & Ibrahim, S. S. 2018 Synthesis of mesoporous graphite functionalized by nitrogen for efficient removal of safranin dye utilizing rice husk ash; equilibrium studies and response surface optimization. *J. Inorg. Organomet. Polym. Mater.* **28**, 279–294.

Yang, S., Xiao, T., Zhang, J., Chen, Y. & Li, L. 2015 Activated carbon fiber as heterogeneous catalyst of peroxymonosulfate activation for efficient degradation of Acid Orange 7 in aqueous solution. *Sep. Purif. Technol.* **143**, 19–26.

Yusuf, M., Khan, M. A., Otero, M., Abdullah, E. C., Hosomi, M., Terada, A. & Riya, S. 2017 Synthesis of CTAB intercalated graphene and its application for the adsorption of AR265 and AO7 dyes from water. *J. Colloid. Interf. Sci.* **493**, 51–61.

Zhang, J., Shao, X., Shi, C. & Yang, S. 2013 Decolorization of Acid Orange 7 with peroxymonosulfate oxidation catalyzed by granular activated carbon. *Chem. Eng. J.* **232**, 259–265.

Zhang, Q., Chen, J., Dai, C., Zhang, Y. & Zhou, X. 2015 Degradation of carbamazepine and toxicity evaluation using the UV/persulfate process in aqueous solution. *J. Chem. Technol. Biot.* **90**, 701–708.

Ziajka, J. & Pasiuk-Bronikowska, W. 2005 Rate constants for atmospheric trace organics scavenging $SO_4^{\cdot-}$ in the Fe-catalysed autoxidation of S(IV). *Atmos. Environ.* **39**, 1431–1438.

First received 25 October 2018; accepted in revised form 25 March 2019. Available online 5 April 2019